

# Epigenetic Down-Regulation and Suppressive Role of *DCBLD2* in Gastric Cancer Cell Proliferation and Invasion

Mirang Kim,<sup>1,6</sup> Kyung-Tae Lee,<sup>7</sup> Hay-Ran Jang,<sup>1</sup> Jeong-Hwan Kim,<sup>1</sup> Seung-Moo Noh,<sup>2</sup> Kyu-Sang Song,<sup>3</sup> June-Sik Cho,<sup>4</sup> Hyun-Yong Jeong,<sup>5</sup> Seon-Young Kim,<sup>1</sup> Hyang-Sook Yoo,<sup>1</sup> and Yong Sung Kim<sup>1,6</sup>

<sup>1</sup>Functional Genomics Research Center, KRIBB; Departments of <sup>2</sup>General Surgery, <sup>3</sup>Pathology, <sup>4</sup>Diagnostic Radiology, and <sup>5</sup>Internal Medicine, College of Medicine, Chungnam National University; <sup>6</sup>Department of Functional Genomics, University of Science and Technology, Yuseong-gu, Daejeon, Korea; and <sup>7</sup>Division of Animal Genomics and Bioinformatics, National Livestock Research Institute, Gwonseon-gu, Suwon, Korea

## Abstract

The promoter region of *Discoidin, CUB and LCCL domain containing 2 (DCBLD2)* was found to be aberrantly methylated in gastric cancer cell lines and in primary gastric cancers, as determined by restriction landmark genomic scanning. *DCBLD2* expression was inversely correlated with *DCBLD2* methylation in gastric cancer cell lines. Treatment with 5-aza-2'-deoxycytidine and trichostatin A partially reversed *DCBLD2* methylation and restored gene expression in *DCBLD2*-silenced cell lines. In an independent series of 82 paired gastric cancers and adjacent normal tissues, *DCBLD2* expression was down-regulated in 79% of gastric cancers as compared with normal tissues as measured by real-time reverse transcription-PCR. Pyrosequencing analysis of the *DCBLD2* promoter region revealed abnormal hypermethylation in gastric cancers, and this hypermethylation was significantly correlated with down-regulation of *DCBLD2* expression. Furthermore, ectopic expression of *DCBLD2* in gastric cancer cell lines inhibited colony formation in both anchorage-dependent and anchorage-independent cultures and also inhibited invasion through the collagen matrix. These data suggest that down-regulation of *DCBLD2*, often associated with promoter hypermethylation, is a frequent event that may be related to the development of gastric cancer. (Mol Cancer Res 2008;6(2):222–30)

## Introduction

Advances in diagnostic and treatment technologies for gastric cancer have resulted in excellent long-term survival, but gastric cancer remains the second most common cause of cancer-related death worldwide (1). The molecular mechanisms underlying gastric cancer development and progression remain poorly understood. DNA methylation, associated with histone modification, is a key mechanism to inhibit the expression of tumor suppressor genes, metastasis suppressor genes, angiogenesis inhibitors, and other genes involved in tumor progression (2, 3). DNA methylation markers can be applied in cancer risk assessment and in the early detection, prognosis, and prediction of response to cancer therapy (4–6). To identify novel epigenetic targets in gastric cancer, we have studied global DNA methylation patterns in gastric cancer cell lines and gastric cancer tissues using restriction landmark genomic scanning (RLGS). RLGS is a highly reproducible two-dimensional gel electrophoresis of genomic DNA that allows the simultaneous assessment of more than 2,000 loci when the methylation-sensitive enzyme *NotI* is used as the landmark enzyme (7–10).

In this study, we used RLGS to identify *DCBLD2* as a novel epigenetic target in gastric cancer. *DCBLD2* (also known as ESDN or CLCP1) is a transmembrane protein first isolated from coronary artery cells, and its domain structure is similar to that of neuropilins (11, 12). The neuropilins were identified as isoforms of a specific vascular endothelial growth factor receptor (13), and soluble neuropilin-1 functions as an antagonist to vascular endothelial growth factor-165 and inhibits tumor angiogenesis and progression (14). The neuropilins are also receptors for axon guidance factors called semaphorins (15, 16), and some semaphorins, such as SEMA3B and SEMA3F, have been classified as tumor suppressors (17, 18). *DCBLD2* is considered to play a role in regulation of cell proliferation. *DCBLD2* overexpression leads to a decrease in cell proliferation in 293T cells (11) and vascular smooth muscle cells (19). Although little is known about the function of *DCBLD2*, previous data suggest that *DCBLD2* may play an important role in cancer cell proliferation and metastasis. Here we report that *DCBLD2* is frequently silenced by epigenetic mechanisms in gastric cancer and show its suppressive roles in gastric cancer cell proliferation and invasion.

Received 3/27/07; revised 9/28/07; accepted 11/1/07.

**Grant support:** FG06-11-01 of the 21C Frontier Functional Human Genome Project from the Ministry of Science and Technology of Korea.

The costs of publication of this article were defrayed in part by the payment of page charges. This article must therefore be hereby marked *advertisement* in accordance with 18 U.S.C. Section 1734 solely to indicate this fact.

**Requests for reprints:** Yong Sung Kim, Functional Genomics Research Center, KRIBB, 52 Eoeun-dong, Yuseong-gu, Daejeon 305-806, Korea. Phone: 82-42-879-8110; Fax: 82-42-879-8119. E-mail: yongsung@kribb.re.kr  
Copyright © 2008 American Association for Cancer Research.  
doi:10.1158/1541-7786.MCR-07-0142

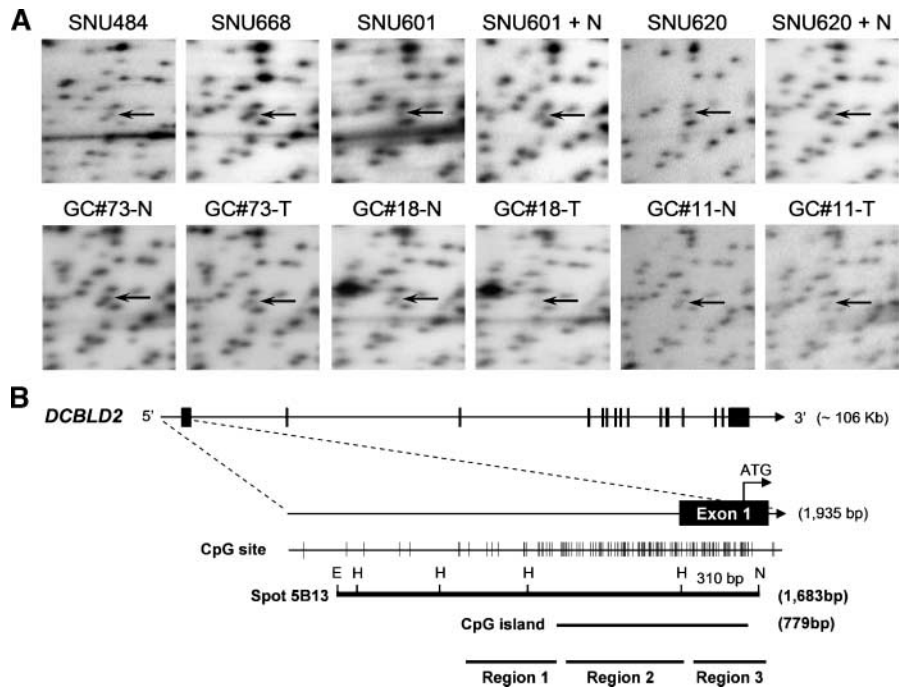


**FIGURE 1.** RLGs analysis and schematic structure of *DCBLD2*. **A.** Representative changes in 5B13 spot intensity in *NotI-EcoRV-HinI* RLGs profiles. Top, spot intensity did not change as compared with neighboring spots in SNU-484 and SNU-668 cell lines, but was decreased in SNU-601 and SNU-620. "+N" indicates that DNA samples were mixed with normal DNA. Bottom, primary gastric cancers (T) or adjacent normal tissues (N) were analyzed by RLGs. Arrow, spot 5B13. **B.** Schematic diagram of *DCBLD2* genomic structure. The map of *DCBLD2* was taken from the UCSC Genome Browser (<http://genome.ucsc.edu>) and shows the position of the coding regions and a CpG island containing 89 CpG sites. The 5B13 clone and the three regions for promoter reporter assay are indicated. E, *EcoRV*; H, *HinI*; N, *NotI*; ATG, start codon.

**Results**

*Decreased DCBLD2 in Gastric Cancer by RLGs Analysis*

We found a DNA spot that was decreased in 5 (SNU-016, SNU-520, SNU-601, SNU-620, and SNU-638) of 11 gastric cancer cell lines tested and in 4 of 15 primary gastric cancers compared with normal tissues profiled by RLGs. Figure 1A shows representative changes in the spot intensity in two gastric cancer cell lines (SNU-601 and SNU-620) and three primary gastric cancers (GC#73, GC#18, and GC#11), but no changes in two gastric cancer cell lines (SNU-484 and SNU-668). The decreased DNA spots corresponded to spot number 5B13 (GenBank accession no. CG465101), which we previously identified by mixing RLGs gels with *NotI*-linked clones (20). The sequence of clone 5B13 was matched to the *NotI/EcoRV* fragment covering the 5' upstream region and exon 1 of *DCBLD2* on human chromosome 3q12.1. The sequence also overlapped with a CpG island at the promoter region of *DCBLD2* (Fig. 1B).<sup>8</sup>

*DCBLD2 Promoter Hypermethylation Is Inversely Correlated with Its mRNA Expression in Gastric Cancer Cell Lines*

To investigate a potential relationship between promoter methylation and down-regulation of *DCBLD2* expression in gastric cancer, we carried out real-time reverse transcription-PCR (RT-PCR) for *DCBLD2* using 11 gastric cancer cell lines. The level of *DCBLD2* expression was relatively low in five cell lines (SNU-016, SNU-520, SNU-601, SNU-620, and SNU-638) with decreased 5B13 spot DNA in RLGs profiles

(Fig. 2D, left). We next assessed the methylation status of each CpG site around the *DCBLD2* CpG island (regions 1-3) by bisulfite sequencing. SNU-216 and SNU-484 cells that expressed normal levels of *DCBLD2* preserved hypomethylated CpG dinucleotides. On the other hand, SNU-601 and SNU-620 cells that expressed *DCBLD2* at low levels showed heavily methylated CpG sites. In addition, these CpG sites were hypomethylated in normal tissues but moderately methylated in paired tumor tissues (Fig. 2A). The methylation pattern of these tumor tissues suggests normal cell contamination, which commonly occurs in dissected tumors. H&E staining confirmed that contaminating normal cells comprised ~60% of the cells in GC#011 and 40% in GC#410 (data not shown). Methylation of region 2 was inversely correlated with *DCBLD2* expression, suggesting that region 2 may be crucial to regulate the transcription level of *DCBLD2*. We tested the three regions around the *DCBLD2* CpG island for promoter activity by luciferase assay in SNU-216 or HeLa cells. Region 2 showed a remarkable increase in transcriptional activity, whereas region 1 and region 3 showed weak activity in both cell lines (Fig. 2B), suggesting that region 2 may contain a sequence critical for *DCBLD2* silencing. Pyrosequencing analysis was also done to quantitate the methylation of seven *DCBLD2* CpG sites at region 2 in 11 gastric cancer cell lines and selected gastric cancer tissues (Fig. 2C). The methylation status measured by pyrosequencing correlated with down-regulation of *DCBLD2* in gastric cancer cell lines (Fig. 2D).

*Restoration of DCBLD2 Expression by Treatment with 5-Aza-2'-Deoxycytidine and Trichostatin A*

We next tested if the expression of *DCBLD2* could be restored by treatment with the DNA methyltransferase inhibitor 5-aza-2'-deoxycytidine (5-aza-dC; ref. 21) or the histone

<sup>8</sup> The master RLGs profile that addresses spot 5B13 can be found at [http://21cgenome.kribb.re.kr/html/2004\\_new/RLGS\\_master/image01.html](http://21cgenome.kribb.re.kr/html/2004_new/RLGS_master/image01.html) (20).

deacetylase inhibitor trichostatin A (TSA; ref. 22). SNU-601, SNU-620, and SNU-638 cells (in which *DCBLD2* mRNA expression is down-regulated and *DCBLD2* promoter is hypermethylated) were treated with 5-aza-dC and/or TSA. After treatment, cells were harvested and analyzed for changes in *DCBLD2* methylation and expression compared with the untreated cells. Pyrosequencing revealed that the CpG sites of *DCBLD2* were partially demethylated by 5-aza-dC and/or TSA in all three cell lines (Fig. 3A). In addition, real-time RT-PCR (Fig. 3B) and Western blotting (Fig. 3C) revealed an increase in *DCBLD2* mRNA and protein expression. TSA was more effective than 5-aza-dC in SNU-620 and SNU-638. Combining 5-aza-dC with TSA had a synergistic effect in all cell lines tested (Figs. 3B and C). These results suggest that *DCBLD2* expression in these gastric cancer cells was regulated by an epigenetic mechanism that includes both DNA methylation and histone deacetylation. Western blotting of primary gastric cancers (which were moderately methylated, as shown in Fig. 2A) and

adjacent normal tissues (which were hypomethylated, as shown in Fig. 2A) revealed that methylation correlated with *DCBLD2* protein expression in primary gastric cancer tissues (Fig. 3D).

#### *DCBLD2 Is Frequently Silenced by CpG Methylation in Primary Gastric Cancers*

We next analyzed *DCBLD2* expression in a series of 82 paired gastric cancers and adjacent normal tissues by real-time RT-PCR. *DCBLD2* expression was significantly reduced in gastric cancers compared with normal tissues ( $P = 0.00011$ ; Fig. 4A). *DCBLD2* expression was decreased in 79% (65 of 82) of gastric cancers compared with normal tissue and was at least 2-fold underrepresented in 51% (42 of 82) of gastric cancers. When the down-regulation of *DCBLD2* was compared within each clinicopathologic category such as tumor depth (early versus advanced gastric cancer), tumor-node-metastasis staging, or Lauren's classification, no significant difference was observed (data not shown).

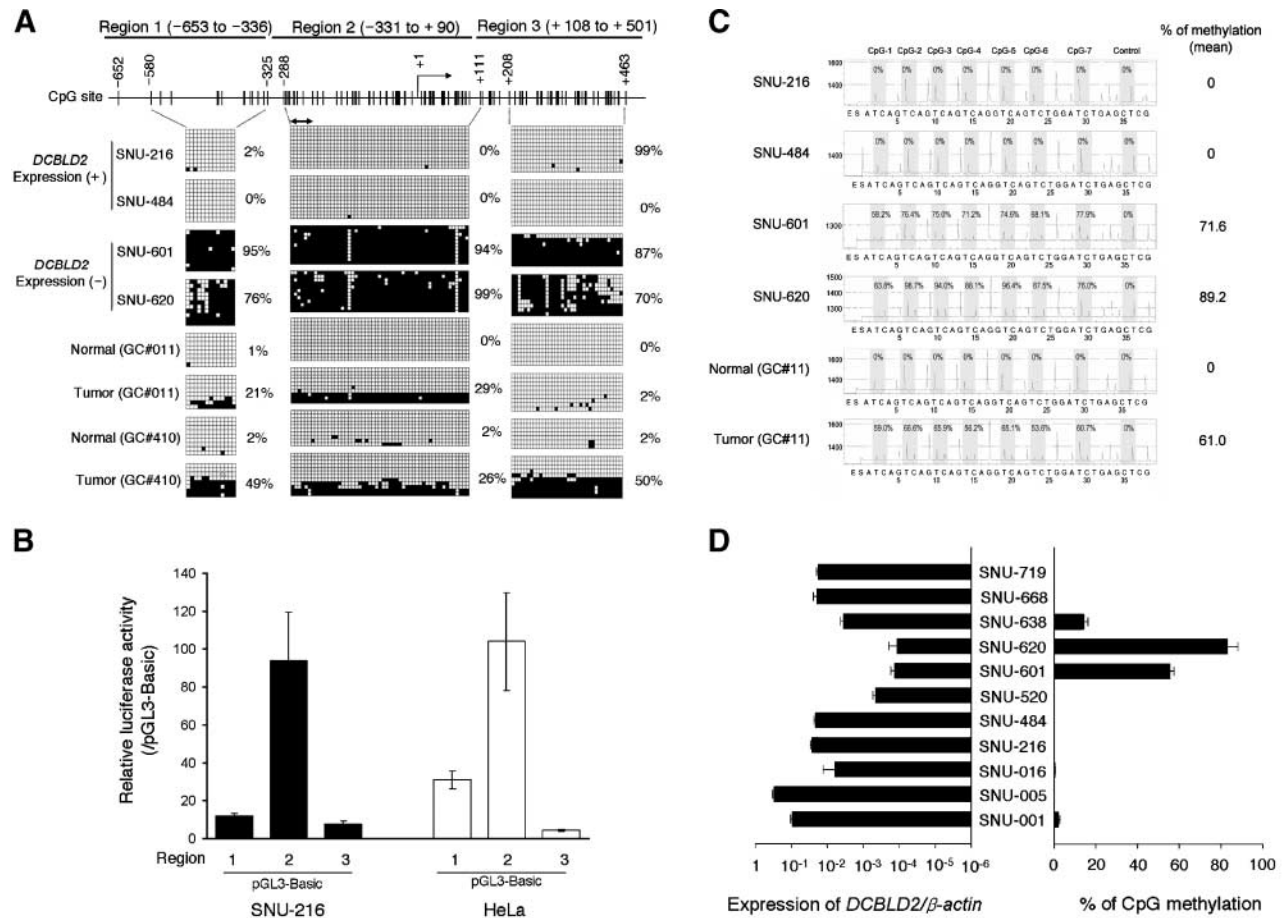


**FIGURE 2.** The relationship between down-regulation of *DCBLD2* mRNA expression and promoter hypermethylation in gastric cancer cell lines. **A**, Bisulfite sequencing analysis of the *DCBLD2* CpG-rich region in *DCBLD2*-expressing and non-*DCBLD2*-expressing gastric cancer cell lines and two pairs of gastric cancer tissues. Each small square box represents a CpG site, and each horizontal line indicates a single clone. Closed and open square boxes, methylated and unmethylated CpG sites, respectively. The arrow on the top indicates CpG sites used for pyrosequencing analysis. **B**, Promoter activity of the *DCBLD2* CpG-rich region. pGL3-Basic empty vector and three constructs containing region 1, 2, or 3 (with 318-, 401-, and 394-bp inserts, respectively) were transfected into SNU-216 and HeLa cells. Luciferase activity was normalized to an internal control. **C**, Pyrogram analysis at seven CpG sites of *DCBLD2*. The expected sequence in this region is YGTTYGGGTYGGGYGGGGTYGYGGGGATTYGAAGTTGG (Y = T or C). The control indicates the complete conversion of cytosine to thymidine in non-CpG cytosines after bisulfite modification. **D**, Correlation between relative *DCBLD2* mRNA expression (left) and methylation status (right). The relative expression value was obtained by real-time RT-PCR and the methylation status by pyrosequencing.

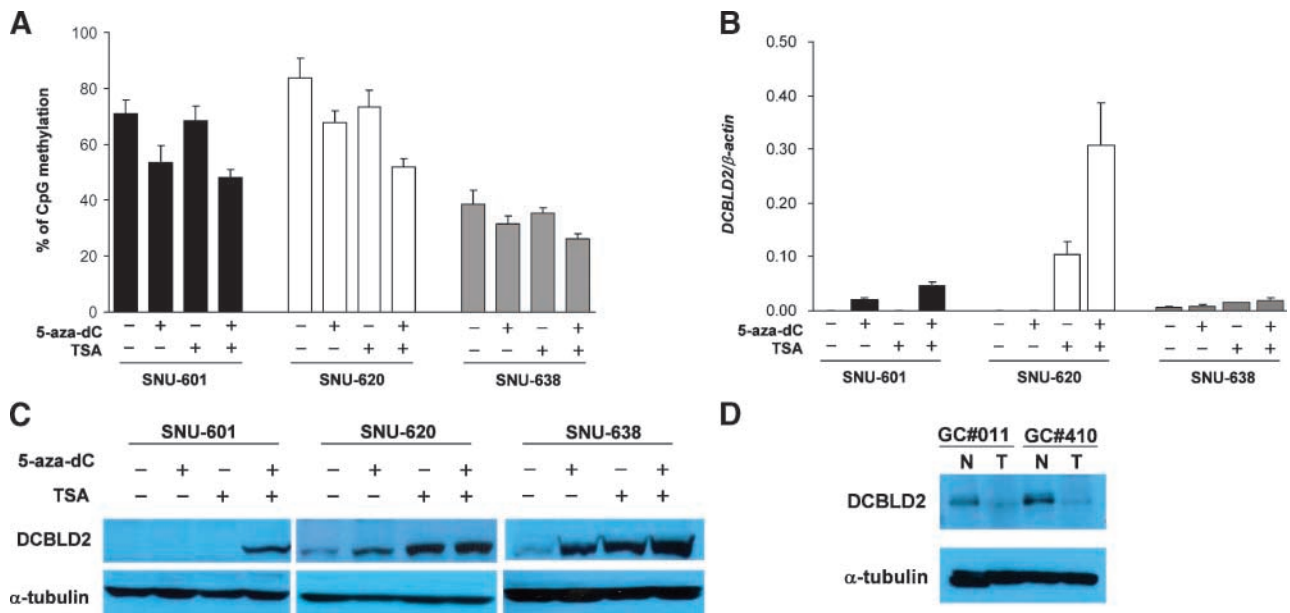


**FIGURE 3.** Restoration of *DCBLD2* expression in SNU-601, SNU-620, and SNU-638 cells after treatment with 5-aza-dC (1  $\mu$ mol/L) for 3 d and/or TSA (500 nmol/L) for 1 d. **A.** *DCBLD2* methylation status was analyzed by pyrosequencing at the end of treatment. **B.** *DCBLD2* expression was analyzed by real-time RT-PCR and was normalized to  $\beta$ -actin expression in each sample. **C.** *DCBLD2* protein expression was analyzed by Western blotting with  $\alpha$ -tubulin as a control. **D.** Western blot of primary gastric cancers, which show moderate methylation of *DCBLD2*, and adjacent normal tissues, which show hypomethylation of *DCBLD2* (Fig. 2A).  $\alpha$ -Tubulin was evaluated as a control.

We next quantitated the methylation status of the seven CpG sites at region 2 by pyrosequencing analysis. The methylation levels in normal tissues were in the range of 0% to 8.6% (mean, 0.7%), whereas those in gastric cancers were in the range of 0% to 73.1% (mean, 12.2%), indicating that overall methylation was higher in gastric cancers ( $P < 0.0001$ ; Fig. 4B). To see if the methylation of *DCBLD2* CpG dinucleotides was associated with *DCBLD2* expression in the clinical samples, we calculated a Pearson's correlation coefficient between relative expression and methylation and inferred its significance by a *t* test. For each pair of tumor and normal samples, we used log 2-transformed ratios between tumor and normal samples as the relative expression and defined methylation change as the difference in methylation between tumor and normal samples. We found a significant negative correlation between relative expression and methylation change ( $r = -0.2728$ ,  $P = 0.0143$ ; Fig. 4C), indicating that decreased *DCBLD2* expression was associated with increased methylation in the clinical samples. When the abnormal methylation was compared within each clinicopathologic category, no difference was observed in any of the chosen variables such as gender, histology, or tumor stage (data not shown). In addition, we found no correlation between methylation and age in either the normal or gastric cancer samples ( $r = -0.0272$ ,  $P = 0.5478$  for normal tissue;  $r = -0.0404$ ,  $P = 0.8039$  for gastric cancers; Fig. 4D). This result indicates that abnormal methylation of *DCBLD2* is a typical cancer-specific (type C), but not age-related (type A), occurrence (23).

*Ectopic Expression of DCBLD2 Suppresses Colony Formation in Gastric Cancer Cell Lines*

Frequent down-regulation of *DCBLD2* in gastric cancers suggests that its dysfunction may play an important role dur-

ing gastric carcinogenesis. To test if ectopic expression of *DCBLD2* suppresses colony formation in gastric cancer cell lines, we transfected a full-length cDNA for *DCBLD2* (pcDNA3-*DCBLD2*-HA) or empty vector (pcDNA3.1) into SNU-216, which endogenously expresses *DCBLD2*, or SNU-601, with reduced *DCBLD2* expression. The expression of *DCBLD2* in transfected cells was confirmed by Western blotting with anti-*DCBLD2* (Fig. 5A). We selected drug-resistant cells for 2 weeks and carried out anchorage-dependent colony formation assays on monolayer cultures. The *DCBLD2*-transfected cells formed fewer colonies than did empty vector-transfected cells in both cell lines (Fig. 5B). Moreover, *DCBLD2*-transfected cells formed fewer colonies than did control cells in an anchorage-independent colony formation assay in soft agar (Fig. 5C). These results suggest that *DCBLD2* suppresses cell proliferation signals in gastric cancer cells.

*DCBLD2 Inhibits Gastric Cancer Cell Invasiveness In vitro*

*DCBLD2* is reportedly up-regulated in a highly metastatic lung cancer cell line (12). In this study, by contrast, in cell lines derived from metastatic gastric cancers, such as SNU-016, SNU-601, SNU-620, and SNU-638 (24, 25), *DCBLD2* expression was down-regulated. To test if *DCBLD2* affects gastric cancer cell invasiveness, we analyzed the pattern of invasion of SNU-601 cells through fibrillar collagen after transfection with pcDNA3-*DCBLD2*-HA or empty vector (Fig. 6A). *DCBLD2*-transfected cells were less invasive through the collagen matrix than control cells ( $P = 0.0016$ ; Fig. 6B), suggesting that *DCBLD2* inhibits the invasiveness of gastric cancer cells.

Downloaded from http://aacrjournals.org/mcr/article-pdf/6/2/222/3141938/222.pdf by guest on 09 February 2023

## Discussion

We report for the first time that *DCBLD2* is a newly defined epigenetic target in gastric cancer related to tumor cell proliferation and invasiveness. We identified decreased representation of *DCBLD2* in 26.7% (4 of 15) of primary gastric cancers as well as in 45.5% (5 of 11) of gastric cancer cell lines by RLGS analysis. Down-regulation of *DCBLD2* expression was associated with promoter hypermethylation in gastric cancer cell lines, and its expression was restored in cells treated with inhibitors of DNA methyltransferase and histone deacetylase. In 51% of primary gastric cancers, *DCBLD2* expression was decreased >2-fold. Furthermore, we frequently detected hypermethylation of the *DCBLD2* promoter region in primary gastric cancers, and this hypermethylation was significantly correlated with *DCBLD2* down-regulation. These results show that *DCBLD2* is frequently down-regulated due to an epigenetic mechanism in gastric cancer, suggesting that this gene may play an important role in gastric carcinogenesis.

A novel molecular phenotype based on promoter CpG hypermethylation in colorectal cancers has been proposed by Toyota et al. (26). Genes with hypermethylated CpG dinucleotides were classified into two types of methylation: age related (type A) and cancer specific (type C). They also found frequent hypermethylation of type C genes in a subset of cancers and

designated this as the CpG island methylator phenotype (CIMP). The CIMP+ phenotype was also identified in 24% to 47% of gastric cancers (23, 27), indicating that multiple promoter regions are methylated in many gastric cancers. We did not observe a correlation between *DCBLD2* methylation and age, indicating that abnormal methylation of *DCBLD2* is a typical type C response according to the previous classification (26).

*DCBLD2* is a single-pass type I transmembrane protein that is highly conserved in mammals (11). *DCBLD2* is expressed in various tissues including skeletal muscle, placenta, heart, colon, ovary, and prostate (12). It is particularly highly expressed in cultured vascular smooth muscle cells and is up-regulated by serum- and platelet-derived growth factor (11). Epidermal growth factor signaling also increases *DCBLD2* and induces tyrosine phosphorylation of *DCBLD2* in A431 human cancer cells (28). It has been suggested that *DCBLD2* up-regulation leads to a decrease in growth rate by reducing the response to growth factors in a negative feedback loop (11, 19). Over-expression of *DCBLD2* inhibits cell proliferation in 293T cells (11) and vascular smooth muscle cells (19), suggesting that the cellular level of *DCBLD2* may play a role in the generation of tumor proliferation signals in gastric epithelial cells. To further characterize *DCBLD2* function *in vitro*, we examined the effect

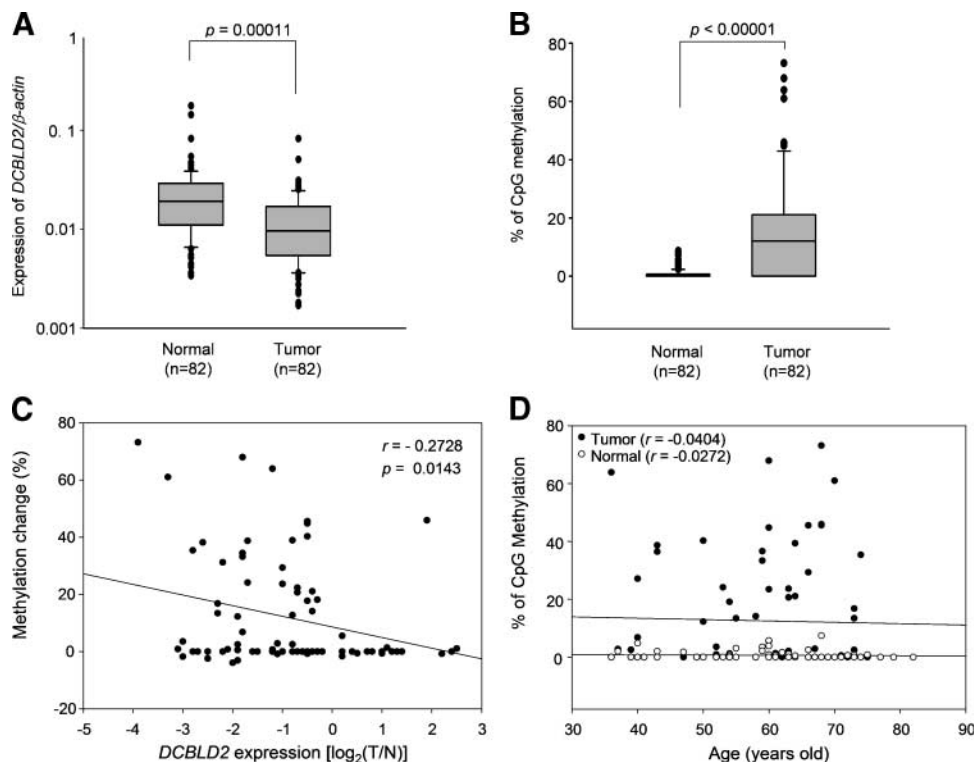


**FIGURE 4.** Quantitation of *DCBLD2* mRNA expression and CpG methylation in primary gastric cancers. **A.** Real-time RT-PCR analysis of *DCBLD2* from 82 primary gastric cancers and adjacent normal tissues. Each mRNA value was normalized to  $\beta$ -actin. *DCBLD2* expression level in gastric cancers was significantly lower than in normal tissues. The box plot analysis shows the median, 25th and 75th percentiles, and outliers. **B.** Pyrosequencing analysis of the samples as in **A.** Methylation of *DCBLD2* CpG dinucleotides in gastric cancers was significantly higher than that in normal tissues. The box plot analysis shows the median, 25th and 75th percentiles, and outliers. **C.** Methylation change and relative expression level of *DCBLD2*. Relative expression values are expressed as the log 2 ratio of tumor to normal. Methylation change is expressed as the difference in methylation between paired tumor and normal tissues (i.e., tumor minus normal). **D.** Methylation change of *DCBLD2* with respect to age. The age (in years) of each patient is plotted against the percentage of CpG sites that were methylated in *DCBLD2*.

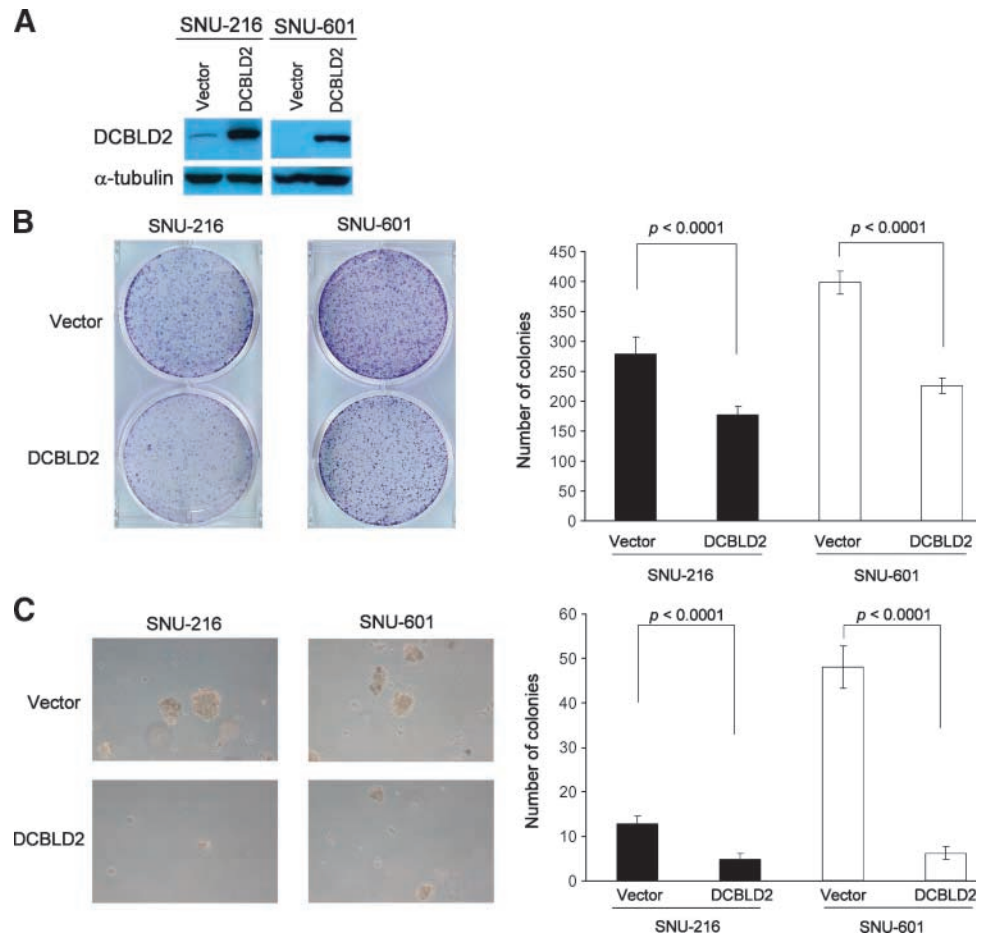


**FIGURE 5.** Effect of ectopic expression of *DCBLD2* on colony formation. **A.** Western blotting with anti-*DCBLD2*. SNU-216 and SNU-601 cells were transfected with pcDNA3-*DCBLD2*-HA (*DCBLD2*) or empty pcDNA3.1 vector (*Vector*) and selected with G418 for 2 wk.  $\alpha$ -Tubulin was used as a control. **B.** Anchorage-dependent colony formation assay in monolayer cultures. Selected SNU-216 and SNU-601 cells were plated on six-well plates at  $1 \times 10^4$  per well. After 2 wk of incubation with G-418, the colonies were stained with crystal violet (*left*). Right, number of colonies formed. Columns, mean of three separate experiments done in duplicate; bars, SD. **C.** Anchorage-independent colony formation assay in soft agar. Colonies were counted 2 wk following seeding in soft agar. Right, number of colonies formed. Columns, mean of three separate experiments done in duplicate; bars, SD.

of *DCBLD2* overexpression in gastric cancer cells. Our results revealed that overexpression of *DCBLD2* strongly inhibited both anchorage-dependent and anchorage-independent cell growth *in vitro*. Furthermore, overexpression of *DCBLD2* significantly inhibited cell invasion through a collagen matrix, suggesting that *DCBLD2* may suppress cell proliferation and invasion signals in gastric cancer.

Taken together, we propose that *DCBLD2* is frequently hypermethylated in gastric cancer and that *DCBLD2* is also related to at least two aspects of gastric carcinogenesis: tumor cell proliferation and invasion. Further studies are needed to evaluate the potential clinical application of hypermethylated *DCBLD2* as a biomarker in gastric cancer. Our results also illustrate the need to study signaling mechanisms involved in *DCBLD2* silencing during tumor progression and metastasis.

## Materials and Methods

### Cell Lines and Tissue Samples

Eleven gastric cancer cell lines established from gastric cancer patients (24, 25) were obtained from the Korean Cell Line Bank<sup>9</sup> and were cultured in RPMI 1640 supplemented with 10% fetal bovine serum and 1% antibiotic-antimycotic

solution (Invitrogen). Frozen gastric cancers paired with normal adjacent tissues were collected from the Stomach Cancer Bank at Chungnam National University Hospital. Specimens were obtained from tumors immediately after resection. Corresponding normal mucosa specimens were at least 3 cm away from the tumor edge. All samples were obtained with informed consent, and their use was approved by the Internal Review Board at Chungnam National University Hospital. For *DCBLD2* expression analysis, 82 paired samples of gastric tumors and normal tissues were used. The samples included 28 tumor-node-metastasis stage I, 13 stage II, 32 stage III, and 9 stage IV tumors, and were obtained from 28 females and 54 males, 36 to 82 years of age (mean, 59 years).

### RLGS Analysis

Genomic DNA was extracted with the phenol-chloroform method (29), and RLGS was done as described (30). Briefly, genomic DNA (5  $\mu$ g) was incubated in the presence of DNA polymerase I (Takara), ddTTP, ddATP, dGTP( $\alpha$ S), and dCTP( $\alpha$ S) to fill in randomly broken ends. The treated DNA was then digested with a methylation-sensitive enzyme, *NotI* (New England BioLabs), end-labeled with [ $\alpha$ -<sup>32</sup>P]dGTP and [ $\alpha$ -<sup>32</sup>P]dCTP using Sequenase (U.S. Biochemical), and subsequently digested with *EcoRV* (New England BioLabs). The labeled DNA (1.5  $\mu$ g) was separated by size on a 0.8% agarose

<sup>9</sup> <http://cellbank.snu.ac.kr/index.htm>



gel at 8 V/cm for 12 h for first-dimensional separation. Thereafter, DNA was digested in the gel with *Hinf*I (New England BioLabs) to further fragment the DNA. The gel was fused with a 5% polyacrylamide gel by adding melted agarose to fill the gap. Second-dimension electrophoresis was carried out at 8 V/cm for 7 h. The gel was dried and exposed to X-ray film. RLGS gels were run for paired samples of primary gastric cancer and adjacent normal tissue. For cell line DNA, RLGS gels were also run in pairs consisting of cell line DNA alone and DNA of the cell line mixed with DNA from normal tissue. The differences between the two profiles of tumor and normal DNA or of cell line and normal DNA were detected as described (31). Once a difference in spot intensity was detected between paired normal and tumor samples or between normal and cell line samples, we compared the spots with the previous master RLGS profile (7) or our RLGS profile (20) to identify their sequences.

#### Real-time RT-PCR Analysis

Total RNA was prepared using the RNeasy kit (Qiagen) according to the manufacturer's guidelines and treated with DNase I (Promega). DNase-treated RNA (5  $\mu$ g) was reverse transcribed with Superscript II reverse transcriptase (Invitrogen) according to the manufacturer's guidelines. Real-time PCR was done in an Exicycler Quantitative Thermal Block (Bioneer). The reverse transcribed product (100 ng) was amplified in a 15- $\mu$ L reaction with 2 $\times$  SYBR Premix EX Taq (Takara) using the *DCBLD2* primer set, 5'-CTCAGCCACTGGTAGGAGGA-3' and 5'-GGCACCTGGTACACCAATTC-3'. The product size was 394 bp. Samples were heated to 95°C for 1 min and then amplified for 45 cycles consisting of 95°C for 30 s, 60°C for 30 s, and 72°C for 30 s. All reactions were then incubated at 72°C for 10 min and cooled to 4°C. The  $\beta$ -actin gene was amplified as a control. Relative quantification of *DCBLD2* mRNA was analyzed by comparative threshold cycle ( $C_T$ ) methods (32).

#### Bisulfite Sequencing Analysis

Genomic DNA (1  $\mu$ g) was modified by sodium bisulfite using the EZ DNA Methylation kit (ZYMO Research)

according to the manufacturer's instructions. Bisulfite-modified DNA was amplified using three primer sets designed to amplify three regions of interest. The primer sequences are 5'-AAAAA-GAGTAGAGAAAATAGGGAAT-3' and 5'-CCTCAACCCA-AACTAATCC-3' (for region 1; 342 bp), 5'-GGGATTAGTTT-GGGTTGAG-3' and 5'-CTTTCACCTACTCCTCCTTC-3' (for region 2; 531 bp), and 5'-GAAGGAGGAGTAGGTGAAAAG-3' and 5'-CACTCACCTTACTAACTCCAA-3' (for region 3; 388 bp). Samples were heated to 95°C for 12 min and then amplified for 35 cycles consisting of 95°C for 45 s, 55°C for 35 s, and 72°C for 60 s. All reactions were then incubated at 72°C for 10 min and cooled to 4°C. The PCR products were visualized on a 1.5% agarose gel by ethidium bromide staining, purified from the gel using the Qiagen Gel Extraction kit, and cloned using the pGEM-T Easy Vector (Promega). Twelve clones were randomly chosen for sequencing. Complete bisulfite conversion was verified by the fact that <0.01% of the cytosines in non-CG dinucleotides was unconverted in the final sequence.

#### Promoter Reporter Assay

DNA fragments around the *DCBLD2* CpG island were obtained by PCR using primer sets designed to amplify three regions of interest. The primer sequences are 5'-CCGCCA-TAAAAAGAGCAGAG-3' and 5'-AGCCAGCTCGTCAGTG-ACTT-3' (for region 1; 318 bp), 5'-AAGCTTGCTGAGGGCC-CAACAATAAC-3' and 5'-CGCCATGGCGGAGCTAAGGA-ACGTG-3' (for region 2; 401 bp), and 5'-gastric cancer-TCGAGGACTCCGCTTC-3' and 5'-GGAGAAGGAGGAG-GAGTTGG-3' (for region 3; 394 bp). The DNA fragments were inserted into the pGEM-T easy vector (Promega) and confirmed by sequencing. Then, the *Sac*I/*Nco*I (for regions 1 and 3) or *Hind*III/*Nco*I (for region 2) fragment was subcloned into the pGL3-Basic vector (Promega). Each construct or a control empty vector and an internal control pRL-CMV vector (Promega) were transfected into SNU-216 or HeLa cells using Lipofectamine Plus reagent (Invitrogen) according to the manufacturer's protocol. Firefly and *Renilla* luciferase activities were measured 48 h after transfection. Relative luciferase activities were calculated after normalization of the transfection efficiency by *Renilla* luciferase activity.

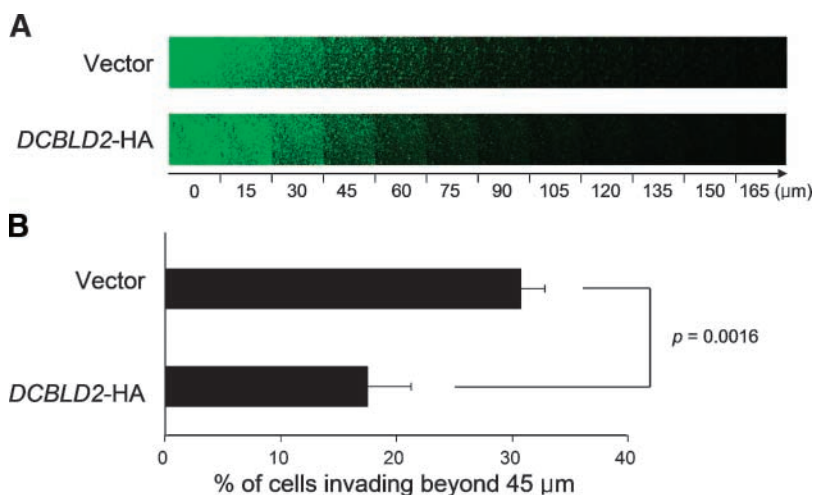


**FIGURE 6.** Three-dimensional invasion analyses through a fibrillar collagen matrix. **A.** SNU-601 cells were transfected with pcDNA3-DCBLD2-HA (*DCBLD2-HA*) or pcDNA3.1 (*Vector*), cultured on fibrillar collagen for 5 d, then stained with calcein and visualized with a confocal microscope using a 10 $\times$  objective. Optical sections (Z sections) were scanned at 15- $\mu$ m intervals moving down from the top of the collagen gel to produce a series of images. Invasion assays were done in triplicate. **B.** Fluorescence intensity values relative to the number of cells on the top layer and at each 15- $\mu$ m layer within the collagen gel was quantified by ImageJ software. Columns, mean percentage of cells that invaded beyond 45  $\mu$ m up to 165  $\mu$ m; bars, SD.

### Pyrosequencing Analysis

The promoter region of *DCBLD2* was amplified using the forward primer 5'-AGTAAGGAGTAAGTTGGGTTTGA-3' and the biotinylated reverse primer 5'-TCCCCTCCACCTT-TAAAA-3', designed by PSQ Assay Design (Biotage AB). The product size was 218 bp. Bisulfite-modified DNA was amplified in a 25- $\mu$ L reaction with the primer set and f-Taq polymerase (Solgent). Samples were heated to 95°C for 5 min and then amplified for 50 cycles consisting of 95°C for 30 s, 58°C for 40 s, and 72°C for 30 s, followed by a final extension step at 72°C for 5 min. Pyrosequencing reactions were done with a sequencing primer (5'-GAGGGTTTAATAA-TAATAGG-3') on the PSQ HS 96A System (Biotage AB) according to the manufacturer's specifications.

### 5-Aza-dC and TSA Treatment

Gastric cancer cells (SNU-601, SNU-620, and SNU-638) were seeded in 10-cm dishes at a density of  $1 \times 10^6$  per dish 1 day before the drug treatment. The cells were treated with 1  $\mu$ mol/L 5-aza-dC (Sigma) every 24 h for 3 days and then harvested. Another culture of cells was treated with 500 nmol/L TSA (Sigma) for 1 day. To test the combined effect of 5-aza-dC and TSA, cells were treated with 1  $\mu$ mol/L 5-aza-dC for 3 days followed by treatment with 250 nmol/L TSA for 1 day. DNA was prepared and tested for reversion of *DCBLD2* methylation by pyrosequencing. Total RNA and protein were prepared and tested for restoration of *DCBLD2* expression by real-time RT-PCR and Western blotting.

### Transfection and Colony Formation Assay

pcDNA3-DCBLD2-HA is a COOH-terminal hemagglutinin (HA)-tagged full-length *DCBLD2* expression vector that was constructed in the laboratory of Dr. T. Takahashi (12). For colony formation assays in a monolayer culture, equimolar amounts of pcDNA3-DCBLD2-HA or empty control vector (pcDNA 3.1) were transfected into SNU-216 or SNU-601 cells in six-well plates using Lipofectamine Plus reagent (Invitrogen) according to the manufacturer's protocol. The cells were selected with G418 (300  $\mu$ g/mL) for 2 weeks and then plated into fresh six-well plates at  $1 \times 10^4$  per well. After 2 weeks of incubation with G418, colonies were stained with crystal violet and counted. To investigate colony formation in soft agar, cells were transfected and selected as above. The cells were suspended in RPMI containing 0.3% agarose (Sigma, A-9045), 10% fetal bovine serum, and 300  $\mu$ g/mL G418 and layered on RPMI containing 0.6% agarose, 10% fetal bovine serum, and G418 in a six-well plate. Colonies were photographed and counted after 2 weeks of incubation at 37°C. The expression of *DCBLD2* was confirmed by Western blotting with anti-*DCBLD2* (Sigma).  $\alpha$ -Tubulin was analyzed as a control in the same samples.

### Invasion Assay

Invasion assays were done as described (33). Fibrillar collagen type I gels (1 mg/mL) were prepared by neutralizing

a solution of collagen type I (Vitrogen 100, Cohesion) in 8- $\mu$ m-pore, 6.5-mm polycarbonate transwells (Corning) for 1 h at 37°C. SNU-601 cells ( $4 \times 10^4$ ) transfected with pcDNA3.1 or pcDNA3-DCBLD2-HA in RPMI containing 0.2% fetal bovine serum were seeded on top of the collagen gel. Transwell inserts were placed in RPMI supplemented with 10% fetal bovine serum and 30 ng/mL EGF to provide a chemotactic gradient and were incubated at 37°C for 5 days. Whole cells were stained with 4  $\mu$ mol/L calcein-acetoxymethyl ester (Invitrogen C1430) in serum-free RPMI and visualized by confocal microscopy using a 10 $\times$  objective. Optical sections (Z sections) were scanned at 15- $\mu$ m intervals moving down from the top of the collagen gel. The quantification of invading cells at each section was evaluated using ImageJ software from the Research Service Branch website of the NIH.<sup>10</sup>

### Statistical Analysis

The Student unpaired *t* test was used to test differences in *DCBLD2* expression or *DCBLD2* promoter methylation between primary gastric cancers and adjacent normal tissues. Results for which *P* < 0.05 were considered significant. Correlation between the level of *DCBLD2* expression and *DCBLD2* CpG methylation or between methylation and aging was determined using the Pearson's correlation coefficient (*r*), and its significance was inferred from a *t* test using a *t* value calculated from the following formula:  $t = r[(n - 2) / (1 - r^2)]^{1/2}$  with *n* - 2 degrees of freedom. The clinicopathologic factors in various groups of patients with positive or negative *DCBLD2* expression and positive or negative *DCBLD2* promoter methylation were compared using the  $\chi^2$  test.

### Acknowledgments

We thank Dr. T. Takahashi (Nagoya University Graduate School of Medicine, Nagoya, Japan) for the HA-tagged *DCBLD2* expression vector.

### References

- Parkin DM, Bray F, Ferlay J, Pisani P. Global cancer statistics 2002. *CA Cancer J Clin* 2005;55:74–108.
- Baylin SB, Ohm JE. Epigenetic gene silencing in cancer—a mechanism for early oncogenic pathway addiction? *Nat Rev Cancer* 2006;6:107–16.
- Ushijima T. Detection and interpretation of altered methylation patterns in cancer cells. *Nat Rev Cancer* 2005;5:223–31.
- Laird PW. The power and the promise of DNA methylation markers. *Nat Rev Cancer* 2003;3:253–66.
- Maier S, Dahlstroem C, Haefliger C, Plum A, Piepenbrock C. Identifying DNA methylation biomarkers of cancer drug response. *Am J Pharmacogenomics* 2005;5:223–32.
- Egger G, Liang G, Aparicio A, Jones PA. Epigenetics in human disease and prospects for epigenetic therapy. *Nature* 2004;429:457–63.
- Costello JF, Fruhwald MC, Smiraglia DJ, et al. Aberrant CpG-island methylation has non-random and tumour-type-specific patterns. *Nat Genet* 2000;24:132–8.
- Ando Y, Hayashizaki Y. Restriction landmark genomic scanning. *Nat Protoc* 2006;1:2774–83.
- Rush LJ, Plass C. Restriction landmark genomic scanning for DNA methylation in cancer: past, present, and future applications. *Anal Biochem* 2002;307:191–201.
- Yoshikawa H, de la Monte S, Nagai H, Wands JR, Matsubara K, Fujiyama A. Chromosomal assignment of human genomic NotI restriction fragments in a two-dimensional electrophoresis profile. *Genomics* 1996;31:28–35.
- Kobuke K, Furukawa Y, Sugai M, et al. ESDN, a novel neuropilin-like membrane protein cloned from vascular cells with the longest secretory signal

<sup>10</sup> <http://rsb.info.nih.gov/>



- sequence among eukaryotes, is up-regulated after vascular injury. *J Biol Chem* 2001;276:34105–14.
12. Koshikawa K, Osada H, Kozaki K, et al. Significant up-regulation of a novel gene, CLCP1, in a highly metastatic lung cancer subline as well as in lung cancers *in vivo*. *Oncogene* 2002;21:2822–8.
  13. Soker S, Fidler H, Neufeld G, Klagsbrun M. Characterization of novel vascular endothelial growth factor (VEGF) receptors on tumor cells that bind VEGF165 via its exon 7-encoded domain. *J Biol Chem* 1996;271:5761–7.
  14. Gagnon ML, Bielenberg DR, Gechtman Z, et al. Identification of a natural soluble neuropilin-1 that binds vascular endothelial growth factor: *in vivo* expression and antitumor activity. *Proc Natl Acad Sci U S A* 2000;97:2573–8.
  15. Kolodkin AL, Levengood DV, Rowe EG, Tai YT, Giger RJ, Ginty DD. Neuropilin is a semaphorin III receptor. *Cell* 1997;90:753–62.
  16. He Z, Tessier-Lavigne M. Neuropilin is a receptor for the axonal chemorepellent Semaphorin III. *Cell* 1997;90:739–51.
  17. Tse C, Xiang RH, Bracht T, Naylor SL. Human Semaphorin 3B (SEMA3B) located at chromosome 3p21.3 suppresses tumor formation in an adenocarcinoma cell line. *Cancer Res* 2002;62:542–6.
  18. Xiang R, Davalos AR, Hensel CH, Zhou XJ, Tse C, Naylor SL. Semaphorin 3F gene from human 3p21.3 suppresses tumor formation in nude mice. *Cancer Res* 2002;62:2637–43.
  19. Sadeghi MM, Esmailzadeh L, Zhang J, et al. ESDN is a marker of vascular remodeling and regulator of cell proliferation in graft arteriosclerosis. *Am J Transplant* 2007;7:2098–105.
  20. Kim J-H, Lee K-T, Kim H-C, et al. Cloning of *Nor1*-linked DNA detected by restriction landmark genomic scanning of human genome. *Genomics & Informatics* 2006;4:1–10.
  21. Jones PA, Taylor SM. Cellular differentiation, cytidine analogs and DNA methylation. *Cell* 1980;20:85–93.
  22. Yoshida M, Kijima M, Akita M, Beppu T. Potent and specific inhibition of mammalian histone deacetylase both *in vivo* and *in vitro* by trichostatin A. *J Biol Chem* 1990;265:17174–9.
  23. Toyota M, Ahuja N, Suzuki H, et al. Aberrant methylation in gastric cancer associated with the CpG island methylator phenotype. *Cancer Res* 1999;59:5438–42.
  24. Park JG, Frucht H, LaRocca RV, et al. Characteristics of cell lines established from human gastric carcinoma. *Cancer Res* 1990;50:2773–80.
  25. Park JG, Yang HK, Kim WH, et al. Establishment and characterization of human gastric carcinoma cell lines. *Int J Cancer* 1997;70:443–9.
  26. Toyota M, Ahuja N, Ohe-Toyota M, Herman JG, Baylin SB, Issa JP. CpG island methylator phenotype in colorectal cancer. *Proc Natl Acad Sci U S A* 1999;96:8681–6.
  27. Oue N, Oshimo Y, Nakayama H, et al. DNA methylation of multiple genes in gastric carcinoma: association with histological type and CpG island methylator phenotype. *Cancer Sci* 2003;94:901–5.
  28. Chen Y, Low TY, Choong LY, et al. Phosphoproteomics identified Endofin, DCBLD2, and KIAA0582 as novel tyrosine phosphorylation targets of EGF signaling and Iressa in human cancer cells. *Proteomics* 2007;7:2384–97.
  29. Birren B, Green E, Klapholz S, Myers R, Roskams J. *Genome analysis: a laboratory manual*. New York: Cold Spring Harbor Laboratory Press; 1997. p. 1–15.
  30. Hatada I, Hayashizaki Y, Hirotsune S, Komatsubara H, Mukai T. A genomic scanning method for higher organisms using restriction sites as landmarks. *Proc Natl Acad Sci U S A* 1991;88:9523–7.
  31. Kim SK, Jang HR, Kim JH, et al. The epigenetic silencing of LIMS2 in gastric cancer and its inhibitory effect on cell migration. *Biochem Biophys Res Commun* 2006;349:1032–40.
  32. Johnson MR, Wang K, Smith JB, Heslin MJ, Diasio RB. Quantitation of dihydropyrimidine dehydrogenase expression by real-time reverse transcription polymerase chain reaction. *Anal Biochem* 2000;278:175–84.
  33. Carragher NO, Walker SM, Scott Carragher LA, et al. Calpain 2 and Src dependence distinguishes mesenchymal and amoeboid modes of tumour cell invasion: a link to integrin function. *Oncogene* 2006;25:5726–40.